[Frontiers in Bioscience, Elite, 5, 643-652, January 1, 2013]

The carbonate ion in hydroxyapatite: Recent X-ray and infrared results

Michael E. Fleet

Department of Earth Sciences, University of Western Ontario, London, Ontario N6A 5B7

TABLE OF CONTENTS

1. ABSTRACT

The location and orientation of the carbonate ion in the channel (A) and phosphate (B) positions of hydroxyapatite (CHAP) have been investigated by single-crystal X-ray structure and Fourier transform infrared (FTIR) spectroscopy, using crystals synthesized at high pressure. The type A carbonate ion is oriented in the apatite channel with two oxygen atoms close to the *c*-axis and the B carbonate ion is located near a sloping face of the substituted phosphate tetrahedron. Close comparison of FTIR and X-ray structure results shows that a Na-bearing CHAP containing approximately equal amounts of A and B carbonate ions is a realistic model for the overall crystal structure of biological apatite. However, the absence of distinct OH stretch and OH libration bands indicates that the hydroxyl content of biological apatite is disordered in respect to its orientation and precise location both in the channel and elsewhere in the structure.

2. INTRODUCTION

The apatite-type structure is adopted by numerous inorganic compounds of general formula $M1_2M2_3(BO_4)_3X$, where M1 and M2 are large cations, B metalloids and X halides or oxy-anions (1). Apatite minerals of interest in geochemistry are dominantly solid solutions of hydroxyapatite [HAP; ideally $Ca_{10}(PO_4)_6(OH)_2$; $Z = 1$], fluorapatite [FAP; $Ca_{10}(PO_4)_6F_2$] and chlorapatite [CLAP; $Ca_{10}(PO_4)_6Cl_2$], where Z is the number of formula units per unit cell. These minerals sequester phosphorus, rare earth elements, actinides, and volatile elements in the Earth's crust and mantle. Carbonate-bearing HAP (presently abbreviated as CHAP) is the dominant inorganic component in the hard tissue of vertebrates, accounting for up to about 65 % of cortical bone and 97 % of dental enamel (2). Fluoride hosted by CHAP is the important anticaries component of dental enamel (2-3), and CHAP and carbonated FAP (CFAP) are

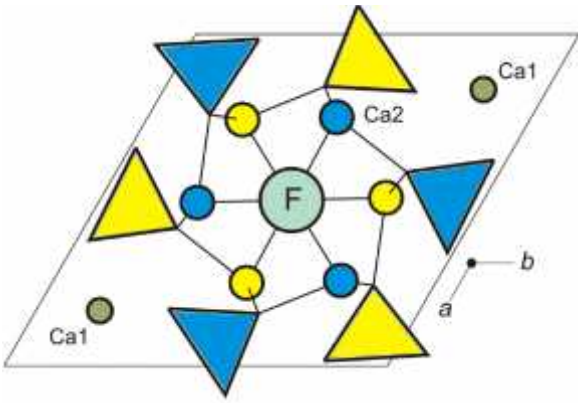

Figure 1. Structure of fluorapatite showing triclusters of Ca2 cations in channel wall: circles and triangles are Ca2 and PO_4 groups, respectively, at height z = 1/4 (yellow) and z = 3/4 (blue); F anion is located on c-axis and unit-cell outline is displaced by (-0.5, -0.5, 0.0).

the dominant minerals in phosphorites (4). The structural role of the carbonate ion in biological apatite has a critical bearing on the growth and strength of bone (5) and bone physiology, as well as the development of bone prostheses.

Natural calcium apatites all have hexagonal symmetry with space group $P6_3/m$, although pure, end-member HAP and CLAP crystallize in the monoclinic space group $P2_1/b$ (6). The hexagonal crystal structure is well known. Apatite is an orthophosphate: isolated PO_4 tetrahedra centered at a height z = (1/4, 3/4) along the c-axis are linked by Ca1 in ninefold (6+3) coordination and Ca2 in an irregular sevenfold (6+1) coordination. A prominent feature of the structure is the large c-axis channel that accommodates the X anion component (F,OH,Cl) and is defined by triclusters of Ca2 cations at z = (1/4, 3/4) (Figure 1). In FAP, the F anion is located on the c-axis at z = (1/4, 3/4) in the center of a tricluster of Ca2 cations. Whereas, larger or more bulky X anions like OH in HAP and Cl in CLAP are displaced along the c-axis and have split atom positions with occupancies of 0.5: e.g. the hydroxyl oxygen is at z = +/-(0.198, 0.302) in HAP and the much larger Cl anion is displaced further at z = +/-(0.432, 0.068) in CLAP (7). Thus, the coordination of the X anion corresponds to ideal equilateral triangular geometry in FAP but is near octahedral in CLAP.

The structural role of carbonate in HAP and FAP has been investigated extensively by X-ray powder and single-crystal and neutron powder diffraction methods (8-13), as well as by infrared, Raman and nuclear magnetic resonance spectroscopy (e.g. 11,14-24) and theoretical simulations (25-26). It has been established that the carbonate ion can be accommodated either in the c-axis structural channel or as a substituent for the phosphate group: the former carbonate is known as type A and the latter as type B. Biological apatite, CHAP minerals and many inorganic preparations of CHAP generally contain detectable amounts of both A and B carbonate ions (AB-CHAP). End-member A-CHAP may be synthesized by annealing HAP at high temperature under a moderate pressure of CO_2 (13,15), and near end-member B-CHAP is prepared by aqueous precipitation, where the channel location for carbonate is blocked by the preferential entry of OH and molecular H_2O species (11,16).

The detailed crystal structure of biological CHAP remains elusive, incisive research being frustrated by: (1) the limited amount of carbonate substituted into the basic HAP structure; (2) small (nanoscale) crystal size of biological apatite and apatite precipitated inorganically from aqueous solution, as well as of francolite from phosphorites; (3) low degree of crystallinity; (4) weak and overlapped electron density of the carbonate ion oxygen atoms; and (5) ambiguous chemical spectra. These problems are largely circumvented in this study for inorganic CHAP crystallized from carbonate-rich melts at high temperature and pressure (1000-1500°C, 0.5-4.0 GPa).

3. MATERIALS AND METHODS

Single crystals of carbonate-bearing apatites were prepared by direct reaction of analytical grade reagents at high pressure and temperature, using an end-loaded piston cylinder apparatus for experiments at >1.0 GPa and a Depths of the Earth Company Quickpress at ≤1.0 GPa (Table 1). Starting materials were: $Ca_2P_2O_7$, $CaCO_3$ and CaO for Na-free CHAP (22,27-29); $CaHPO_4$, Na_2CO_3, $Ca(OH)_2$, and $CaCO_3$ for Na-bearing CHAP (30); $Ca_2P_2O_7$, CaF_2, $CaCO_3$, and Na_2CO_3 ± CaO for CFAP (31); and $Ca_2P_2O_7$, $CaCl_2$, $CaCO_3$, and Na_2CO_3 for CCLAP (32). Calcium pyrophosphate, CaO and CaF_2 were dried at 1000°C for 12 h, Na_2CO_3, $Ca(OH)_2$ and $CaCO_3$ were dried at 200°C and 1 atm for 48 h, and anhydrous $CaCl_2$ was prepared by heating $CaCl_2.2H_2O$ at 300°C for 24 h. All starting compositions were mixed and ground under acetone in an agate mortar, and stored at 110°C for later use. In addition, furnace parts were previously fired at 1000°C in air. For each experiment, the starting mixture was encapsulated in a sealed platinum tube, with a diameter of 5 mm and a height of 10 mm, which was separated by crushable MgO tubing from a graphite sleeve. All experiments were quenched at pressure by switching off the furnace.

Products were characterized by optical microscopy, powder X-ray diffraction (Rigaku D/MAX-B rotating anode system; Co *K*alpha X-radiation), electron probe micro-analysis (EPMA; JEOL JXA-8600, using a lead stearate spectrometer crystal for carbon), and Fourier transform infrared (FTIR) spectroscopy (Nicolet Nexus 670 FTIR spectrometer). The infrared spectra were obtained for both hand-separated crystals and bulk samples using KBr pellets. About 10 mg of apatite crystal product was first ground to a powder, then diluted in an agate mortar with 1g of KBr and ground under an infrared heating lamp to a grain size <25 micrometers. Transparent pellets were made under vacuum at a pressure of 200 kg/cm^2. The temperature of the sample under the infrared heating lamp was 60±5°C, and the exposure time was typically 10 to 30 minutes. Single crystals were evaluated for X-ray structure analysis by optical microscopy. Single crystal measurements were made at room temperature and pressure with a Bruker-

Table 1. Synthesis experiments and amounts of Na, A and B carbonate (*pfu*[1])

		T	P	EPMA	X-ray structure			FTIR
Apatite	Expt	(°C)	(GPa)	Na	A	B	B/A	B/A
Na-free apatites								
B-CHAP	PC17	1400	3.0	-	-	0.17(2)	-	1.3
A-CHAP	PC16	1400	4.0	-	0.14(3)	-	-	0.3
	PC71	1400	2.0	-	0.75	0.11(2)	0.2	0.2
AB-CHAP	PC18	1400	3.0	-	1.08(8)	0.49(2)	0.5	0.5
	PC55	1400	3.0	-	1.09(4)	0.56(2)	0.5	0.4
Na-bearing apatites								
AB-CHAP	LM005	1200	0.5	0.87(3)	1.00(5)	0.77(3)	0.8	0.9
	LM006	1200	1.0	0.35(4)	0.52(3)	0.38(2)	0.7	0.8
AB-CCLAP	LM169	1350	1.0	0.40(4)	0.37(3)	0.57(2)	1.5	1.5
	LM171	1200	1.0	0.39(3)	0.46(4)	0.58(3)	1.3	1.6
	LM173	1000	1.0	0.39(5)	0.42(3)	0.57(2)	1.4	1.4
AB-CFAP	LM130	1250	1.0	0.09(3)	0.08(3)	0.23(1)	2.9	2.6
	LM136	1250	1.0	0.09(3)	0.16(3)	0.21(2)	1.3	1.2
	LM142	1150	1.0	0.11(5)	0.14(3)	0.23(1)	1.6	1.5

[1] *pfu* is per formula unit $[Ca_{10}(PO_4)_6X_2]$.

Nonius Kappa CCD diffractometer and graphite-monochromatized Mo *K*alpha X-radiation (50 kV, 32 mA, wavelength = 0.07107 nm). The COLLECT software (33) was used for unit-cell refinement and data collection. The reflection data were processed with SORTAV-COLLECT, using an empirical procedure for absorption correction, and SHELXTL/PC (34). Structure refinements were made with LINEX77 (35). Scattering factors for neutral atomic species and values of the anomalous scattering factors f' and f'' were taken, respectively, from Tables 2.2A and 2.3.1 of the *International Tables for X-ray Crystallography* (36).

4. RESULTS AND DISCUSSION

Crystals of Na-free A-CHAP were trigonal (space group *P*-3), but all other apatites were hexagonal ($P6_3/m$). All apatite crystal products had positionally-disordered distributions of carbonate ions, reflecting the high symmetry of the host crystals.

4.1. Type A carbonate

The type A carbonate ion substitutes for two hydroxyl ions in the apatite channel according to the ideal substitution reaction:

$$[^{A}CO_3 = 2OH] \quad (1)$$

Early infrared study (14) established that the carbonate ion was oriented parallel to the *c*-axis, but other details of its stereochemistry have remained somewhat controversial. Suetsuga *et al.* (9) reported a structure for A-CHAP in space group *P*-6 with the type A carbonate ion oriented with one oxygen atom close to the *c*-axis, but this model was revised recently by Tonegawa *et al.* (13). Their Rietveld powder X-ray diffraction study resulted in a structure with triclinic (*Pb*) symmetry and two independent channel carbonate ions, both oriented with two oxygen atoms close to the monoclinic *c*-axis, in essential agreement with the *P*-3 structure of the present study (27,37).

In CHAP synthesized at high pressure, the carbonate ion is located in the *c*-axis channel by bonds between the carbonate oxygen atoms and Ca2 cations in the channel wall. The high symmetry of the HAP host structure generates six equivalent orientations of the carbonate ion in the apatite channel for space group *P*-3 symmetry and twelve for $P6_3/m$. Since only one orientation can be occupied in any given unit-cell, the maximum average site occupancies are 0.1667 and 0.0833, respectively. In agreement with this expectation, residual electron density maps calculated at discrete heights along the c-axis, for the X-ray structure of A-CHAP with the carbonate atom positions excluded, reveal very weak residual maxima in multiples of six peaks related by sixfold symmetry (Figure 2). The six residual electron density peaks in Figure 2 represent a single outlying oxygen atom of the carbonate ion at a height along the *c*-axis of $z \approx 0.5$, with the other two oxygen atoms and the carbon located close to the *c*-axis at $z \approx +/- 0.339$ and $z \approx 0.5$, respectively (Figure 3a). The plane of the carbonate ion is approximately normal to (001).

Figure 3a shows the local structure of the A carbonate ion of A-CHAP from experiment PC71 (Table 1) after least-squares refinement and optimization of the Ca2-O bond distances by rigid body rotations and displacements of the carbonate ion (27,29). The channel carbonate ion is rotated 13.6 degrees counterclockwise, relative to an ideal structure with the carbonate ion lying on a vertical glide plane, and is canted 8.8 degrees away from the *c*-axis. It is displaced away from the channel wall, positioning the carbon atom near the *c*-axis, to optimize the Ca2-O6 and Ca2-O7 distances. The equilateral triangular geometry of the carbonate ion (with O-O = 0.2219 nm, C-O = 0.1281 nm) remains incompatible with six Ca2-O distances of equal length. Furthermore, the apatite channel cannot accommodate neighboring carbonate ions centred at $z \approx 0.0$ and 0.5. Therefore, the carbonate ions have to be ordered along the channel at $z \approx 0.5$, leaving the channel location at $z \approx 0.0$ vacant and lowering the symmetry of the end-member A-CHAP to *P*-3. In the A-CHAP of experiment PC71, only three-quarters of the channel locations at $z \approx 0.5$ are occupied by carbonate ions, resulting in site occupancies of only 0.125 for the four carbonate ion atoms. The remaining charge balance is provided by hydroxyl ions. The overall structural adjustments required to accommodate the bulky carbonate ion in the hydroxyapatite channel are complex and include dilation of the channel at *z*

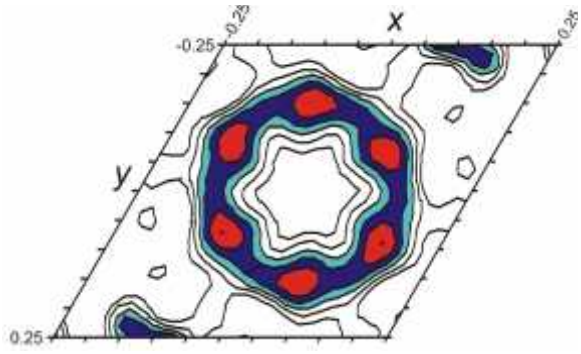

Figure 2. Residual electron density map calculated at height z = 0.5: density >0.5x10^{-3} electrons/nm^3 (red areas) locates off-axis oxygen atom of type A carbonate ion, which is positionally-disordered in the apatite channel.

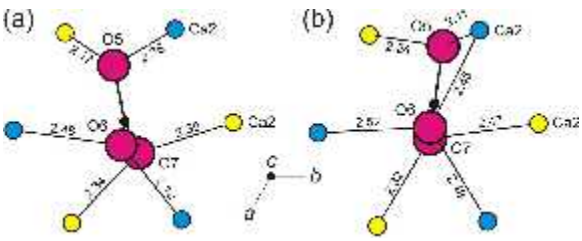

Figure 3. Orientation of type A carbonate ion in *c*-axis channel of: (a) Na-free A-CHAP (PC71), and (b) Na-bearing AB-CHAP (LM005): Ca2 cations in channel wall are at height z = 1/4 (yellow) and z = 3/4 (blue); Ca2-O bond distances are in Angstroms.

≈ 0.5, constriction of the channel at z ≈ 0.0, contraction of the Ca1O$_n$ polyhedron, and rigid body rotation of the PO$_4$ tetrahedron about the P-O1 bond axis (22,27).

Further adjustments are needed to accommodate both type A and type B carbonate ions in AB-CHAP. The *c*-axis channel of Na-bearing AB-CHAP from experiment LM005 (Table 1) is fully occupied by the carbonate ion (Table 1; 30), making analysis of this part of the apatite structure relatively straightforward. The orientation of the carbonate ion is similar to that of the channel carbonate of A-CHAP. However, the plane of the carbonate ion is now rotated clockwise by 13.4 degrees and remains closely parallel to the *c*-axis (tilt angle = 0.0 degrees; Figure 3b).

In Na-free AB-CHAP from experiment PC55 (Table 1), the orientation of the channel carbonate ion is generally similar to that for Na-bearing AB-CHAP from LM005, except that the plane of the carbonate ion is now rotated clockwise by 7.4 degrees and canted 7.3 degrees relative to the *c*-axis (22,28). These similar results for CHAP of diverse compositions are a clear indication that the clockwise rotation of the A carbonate ion in AB-CHAP is related to the introduction of significant amounts of B carbonate. The apatite channel of PC55 also has to accommodate a marginally excess amount of carbonate due to carbonate ions in a second orientation (labeled A2) interpreted to be in a stuffed channel location (28). The presently refined site occupancies for PC55 are 0.042 for A carbonate and 0.049 for A2, compared to a total of 0.083 for one carbonate ion per formula unit (*pfu*). The A2 carbonate ion is also in the vertical orientation but has only one oxygen atom close to the *c*-axis. It is considered to be a high-pressure feature (33) and, therefore, not relevant to a discussion of the structure of biological apatite.

4.2. Type B carbonate

The type B carbonate ion replaces a phosphate group of the HAP structure, using only three of the four oxygen atoms of the PO$_4$ tetrahedron with the fourth oxygen atom generally considered to be lost to the structure. The resulting deficiency in negative charge is compensated in the parallel substitution of Ca by either a monovalent cation or a cation vacancy (Vc), as in the substitution reactions:

$$[Na + {}^{B}CO_3 = Ca + PO_4] \quad (2)$$

and

$$[Vc + {}^{B}CO_3 = 0.5Ca + PO_4] \quad (3)$$

In practice, the charge compensation for type B carbonate is complex and difficult to quantify.

Location of the B carbonate ion in CHAP is problematical and has been controversial (10-12,14,28,30-32). Logically, the B carbonate ion is located in the vicinity of the substituted phosphate group and occupies as many of the phosphate oxygen atom locations as possible. Difficulties here arise from overlap of carbonate and phosphate oxygen atoms in the disordered CHAP structure and the small fraction of phosphate substituted by carbonate in a typical single crystal of CHAP. There are several possible locations for the B carbonate ion, but the most likely ones are derived from the three-membered clusters of oxygen atoms forming the faces of the substituted phosphate tetrahedron. In the hexagonal $P6_3/m$ structure of HAP, two faces of the phosphate tetrahedron are inclined to the *c*-axis and related by the horizontal symmetry plane at z = +/- 0.25 (these are presently referred to as sloping faces) and two are oriented in the vertical plane (Figure 1). In early research, Elliott (14) deduced from polarized infrared spectra that the B carbonate ion in francolite (CFAP) was located close to a sloping face of the substituted phosphate tetrahedron.

Several structure studies have noted that the presence of B carbonate is indicated by significant reduction in the occupancy of the P position (12,38). A linear inverse correlation between formula amounts of B carbonate and phosphorus is observed for the present Na-bearing apatites synthesized at high pressure (Table 1; 30,31,32), with B carbonate estimated from the product of the X-ray structure result for A carbonate and the B/A ratio from the FTIR spectra (see below). This correlation shows that the phosphate position in the apatite structure is fully occupied by randomly distributed (PO$_4$,CO$_3$) groups, thus permitting the calculation of an accurate value for the B carbonate content from the sum (6 - P), where P is the

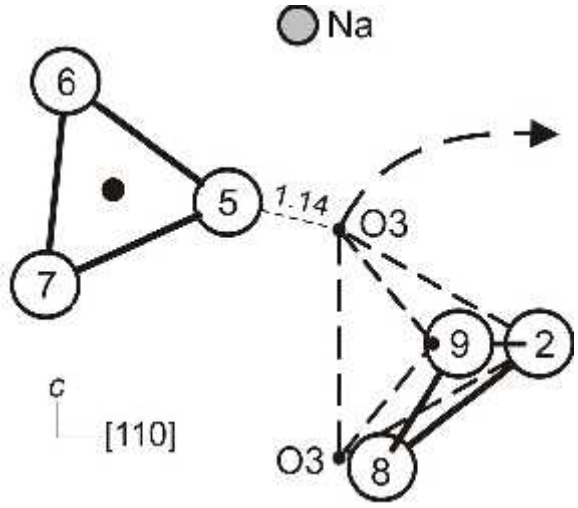

Figure 4. Fragment of structure of Na-bearing AB-CHAP (LM005), showing location of type B carbonate ion (oxygen atoms O2, O8 and O9) close to a sloping face of the substituted PO_4 tetrahedral group.

phosphorus content per formula unit (*pfu*). This was most fortunate because the extensive overlap of phosphate and carbonate oxygen atoms prevented direct quantitative determination of the B carbonate occupancy by the X-ray structure method.

The various studies on high-pressure synthesized CHAP (22,28,30) only detected significant residual electron density consistent with the B carbonate ion in the vicinity of the sloping faces of the substituted phosphate tetrahedron. Residual electron density consistent with a carbon atom was not detected but this was attributed to the weak X-ray scattering efficiency of carbon. However, residual electron density was reported close to the centre of the sloping faces in CHAP precipitated from aqueous solution and studied by neutron powder diffraction (11). In summary, the polarized infrared (14), neutron powder diffraction (11), and present X-ray structure evidence appears to confirm that the most likely location for the B carbonate ion in AB-CHAP is close to one of the sloping faces of the substituted PO_4 tetrahedron.

A preliminary location for the B carbonate ion was obtained from study of Na-free AB-CHAP (22,28), which revealed residual electron density near the oxygen atom position O3. This was interpreted as a probable B carbonate oxygen atom (O8 in Figure 4). The other two oxygen atoms were assumed to be buried in the electron density of O1 and O2. Subsequent X-ray structure analysis of a Na-bearing CHAP (experiment LM005; 30) resulted in a similar orientation for the B carbonate ion with improved resolution of O8, and O9 now resolved separately from O1 in the average structure (Figure 4). This structure confirms that the B carbonate ion in CHAP is located near one of the sloping faces of the substituted phosphate tetrahedron but inclined at an angle of 53 degrees to the mirror plane; i.e. tilted 18 degrees away from the adjacent sloping face. The B carbonate ion is orientated similarly in Na-bearing CCLAP (32). In Na-bearing CFAP it is more closely parallel to the sloping face of the substituted phosphate tetrahedron, being inclined at an angle of only 3.5 degrees (31).

The ratio of Na to A and B carbonate (Na:A:B) is approximately 1:1:1 in CHAP (30), 1:1:1.5 in CCLAP (32), and 1:1:(1.5-2) in CFAP (31; Table 1), and apparently is characteristic of each composition series. These correlations are consistent with the substitution schemes 2 and 3 above, and reveal that Na has an active role in the substitution of carbonate into high-pressure synthesized CHAP. Sodium and vacancies at Ca sites are required for charge balancing the carbonate-for-phosphate substitution after the removal of the fourth oxygen anion. Thus, charge balancing readily explains the coupling of the contents of Na and B carbonate.

However, an explanation for the near-linear 1:1 correlation between Na and A carbonate (Table 1) is not intuitively obvious because Na is not formally required to charge balance the entry of A carbonate, as substitution scheme 1 indicates. However, in the absence of a proximal B carbonate ion, the off-axis oxygen (O5) of the channel A carbonate would be only about 0.11-0.12 nm from an O3 oxygen atom of a phosphate group (Figure 4). And this prohibitively short O5-O3 interaction is eliminated when the O3 oxygen atom in question is removed entirely from the structure (arrow in Figure 4). It seems clear that the B carbonate ion must be located close to the sloping face furthest away from O5, although this structural detail is not resolved in the present refinements of the average structures. Also, a B carbonate ion introduced through substitution scheme 2 must be spatially coupled with an A carbonate ion in the adjacent channel. Logically, charge balance requirements favor placing the Na cation closest to the vacant O3 oxygen site, as indicated in Figure 4. This discussion strongly suggests that the A and B carbonate ions and Na are locally coupled in CHAP as a defect cluster to facilitate charge compensation and minimize the effects of spatial accommodation.

4.3. Infrared spectra

The characteristic infrared bands for carbonate in CHAP occur in the spectral regions 1400-1600 cm^{-1} (asymmetric stretch vibration, nu3; Figure 5) and 873-880 cm^{-1} (out-of-plane bend vibration, nu2; Figure 5). In addition, a weak band for the stretch vibration of structurally-bound OH may be present near 3572 cm^{-1} accompanied by a band of moderate strength near 631 cm^{-1} which is widely attributed to OH libration. The nu3 region of the infrared spectra of AB-CHAP is comprised of complexly overlapped contributions from the A and B carbonate ion species. The nu3 vibration is twofold degenerate for the free carbonate ion but is represented by a doublet in apatite spectra because the degeneracy is lifted for site symmetries lower than trigonal. For Na-free A-CHAP synthesized at high pressure (e.g. experiment PC71 in Table 1), the nu3 region consists of a symmetrical doublet with limbs centred at 1544 and 1461 cm^{-1} (Figure 5a; 27). The spectra of Na-free AB-CHAP from the same series of experiments (e.g. PC55) are complex but six

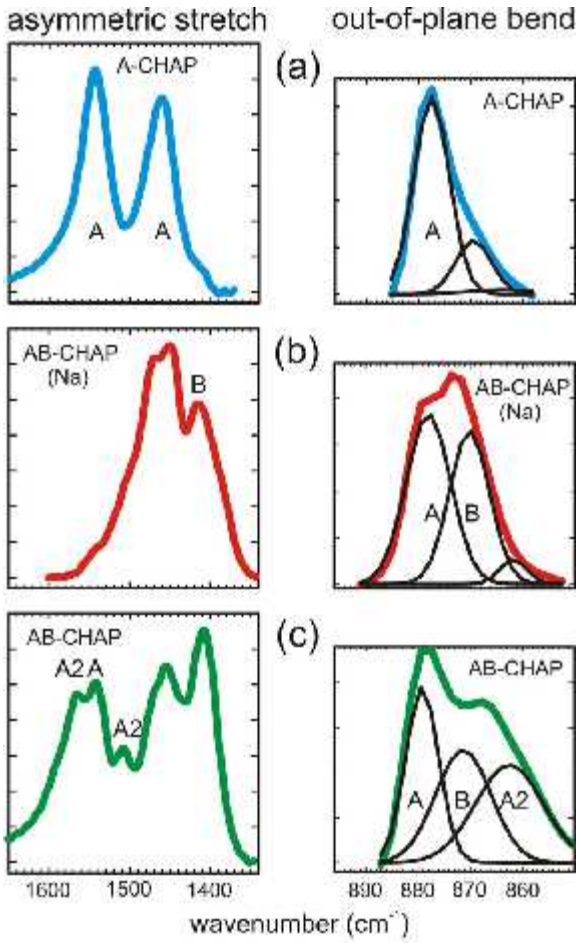

Figure 5. Infrared (FTIR) spectra in the asymmetric stretch (nu3) and out-of-plane bend (nu2) regions for: (a) type A CHAP (PC71), (b) Na-bearing AB-CHAP (LM005), and (c) Na-free AB-CHAP (PC55): note that fitted Gaussian components are shown for nu2 bands.

individual bands are generally recognized by five definite peaks and a prominent shoulder (Figure 5c; 22,28). The strong peak near 1409 cm^{-1} is attributed to one limb of the B carbonate ion doublet (24). The 1540 cm^{-1} band is clearly A carbonate, and the stuffed channel carbonate (A2) is characterized by the doublet bands at 1569 and 1507 cm^{-1}. However, there is no clear basis for proportioning the absorption in the 1470-1455 cm^{-1} interval between A and B carbonate, even with knowledge of the actual (A, A2 and B) site occupancies obtained from the X-ray structures. In the Na-bearing AB-CHAP, AB-CFAP and AB-CCLAP crystals (30,31,32), the nu3 doublet for the A carbonate ion, which is expected to be an important feature from the X-ray structure (Table 1) and infrared nu2 band (Figure 5) results, is seemingly shifted to lower wavenumber into the region normally associated with B carbonate (Figure 5b and 6). These spectra for the synthetic Na-bearing crystals are similar to those of CHAP precipitated from basic solution, dental enamel and cortical bone (2,17,18,39) and previously considered to represent the dominant presence of B carbonate.

In apatite biomaterials, the weak nu2 region is normally deconvoluted to give a singlet band for A carbonate at 878 cm^{-1} and bands for B carbonate at 871 cm^{-1} and 866 cm^{-1} (17,18). The composite nu2 band for laboratory synthesized low-pressure CHAP crystals has components for A1 carbonate at 878-881 cm^{-1} and B carbonate at 870-873 cm^{-1} (8,17). The nu2 spectra for high-pressure synthesized CHAP were interpreted in Fleet (24) by fitting Gaussian components to peaks and prominent shoulders. For Na-free A-CHAP of experiment PC71 and Na-bearing AB-CHAP of LM005, the nu2 spectra are fitted by two bands, one for A carbonate at 878 cm^{-1} and one for B carbonate at 870 cm^{-1} (Figure 5a,b). The nu2 spectrum for Na-free AB-CHAP of PC55 is fitted to three bands, at about 879, 871 and 862 cm^{-1} and assigned to A, B and A2 carbonate, respectively (Figure 5c). The resulting proportions of the A, A2 and B carbonate ion species for experiment PC55 are 31:35:34 and in very good agreement with the proportions of 30:36:34, respectively, obtained for the X-ray structure site occupancies.

The area ratios B/A [or B/(A+A2)] of the fitted nu2 band components are in very good linear agreement with the corresponding quantities calculated from the X-ray structure site occupancies (Figure 7). The proportion of A and B carbonate ions in high-pressure synthesized CHAP is now firmly established by two independent methods, FTIR nu2 band areas and X-ray structure analysis. This agreement also establishes FTIR nu2 band areas as a viable independent method for estimating the proportion of A and B carbonate in CHAP precipitated from aqueous solutions, apatite biominerals and francolites, and it reinforces earlier studies on biological CHAP (17-19).

It is important to note that infrared band positions for the A carbonate ion of AB-CHAP are very sensitive to change in the local stereochemical environment in the apatite channel. We have already seen that the partial substitution of Ca by Na seemingly shifts the high-frequency band of the A carbonate nu3 doublet to lower wavenumber (Figure 5b and 6). Also, the nu3 doublet for the high-pressure A2 carbonate ion, with one oxygen atom near the *c*-axis, is shifted significantly to higher wavenumber (1569 and 1507 cm^{-1}) relative to the A carbonate ion (Figure 5c) and the A2 band for the out-of-plane bend (nu2) vibration is shifted about 17 cm^{-1} to lower wavenumber.

The infrared spectra are also useful in establishing that CO_3 and OH were the only channel anion (X) species present in significant amounts in the synthetic CHAP crystals. In particular, the intensity of the OH libration band, which is located near 631 cm^{-1} on the high-frequency shoulder of the doublet for the phosphate nu4 bend vibration, is directly proportional to the content of structurally-bound OH in the apatite channel (Figure 7). This correlation is relevant only for well-crystallized apatites; i.e. laboratory products annealed at high temperature and most minerals (e.g. 22,38,40-41). Both the sharp band for OH stretch and the OH libration band are absent for synthetic HAP and B-CHAP prepared at low (laboratory) temperature and biological CHAP (e.g.

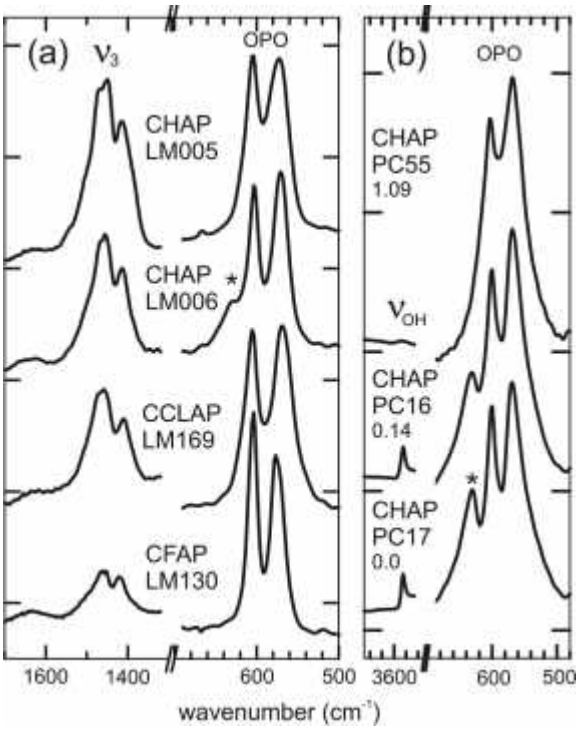

Figure 6. Infrared (FTIR) spectra of selected high-pressure synthesized CHAP: (a) Na-bearing CHAP, showing: (*i*) that the profile of the complex nu3 region is independent of the content of total carbonate, and (*ii*) that absence of the OH libration band (asterisk) indicates that the channel of LM005, LM169 and LM130 is fully occupied by A carbonate +/- halide (Cl,F); and (b) Na-free CHAP, showing that the intensity of the OH libration band (asterisk) is proportional to that of the OH stretch band (nu_{OH}): OPO is phosphate bend; numbers in (b) are content of total A carbonate per formula unit; other details on composition series are given in Table 1

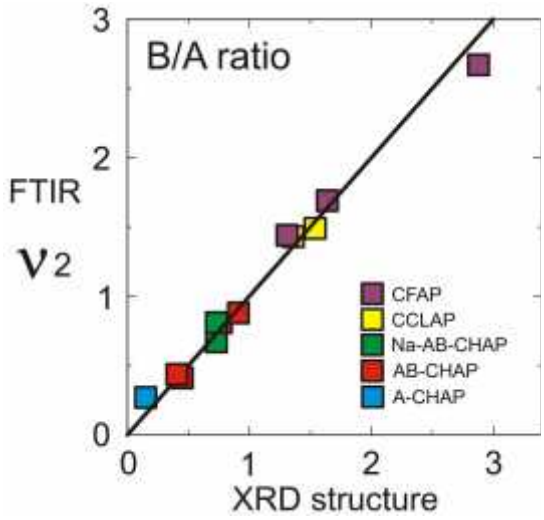

Figure 7. Comparison of the ratio of B carbonate to total A carbonate (B/A) determined by infrared (FTIR) and X-ray structure methods: see Table 1 for details on composition series.

11,39,42-43). This absence is readily attributed to the low degree of crystallinity of HAP and CHAP crystals grown either in aqueous media or *in vivo* and not subsequently annealed. Channel OH and H_2O species are present in these carbonate apatites but are not structurally bound in the apatite channel. Note that, for well crystallized CHAP, CFAP and CCLAP, the absence of the OH stretch and libration bands (Figure 6) indicates that all channel locations are statistically filled with A carbonate ± halide (F,Cl).

The FTIR spectra independently confirm that A and B carbonate ions and Na are coupled locally as a defect cluster in CHAP as depicted in Figure 4. It has been noted above that the nu3 bands of type A carbonate in Na-bearing AB-CHAP are shifted to lower wavenumber and extensively overlap the spectrum of type B carbonate. The resulting characteristic nu3 band profile is surprisingly similar for all Na-bearing carbonate apatite composition series (X = OH,F,Cl) and carbonate contents investigated (30,31-32; present Figure 6). The local environments of the Na cation and A and B carbonate ions are similar in all of these apatites of diverse bulk composition and total carbonate content because these three substituents are present as a defect cluster (Figure 4) common to all of the composition series (Table 1) and randomly distributed within the host apatite structures. It is recognized that charge compensation through the introduction of vacancies at large cation sites (substitution scheme 3) may involve a separate (or more complex) defect cluster in CFAP and CCLAP, because both of these apatite series have molar (B/Na) > 1 (Table 1), although this is not reflected by change in their nu3 band profiles.

4.4 Biological apatite

The Na-bearing AB-CHAP of experiment LM006 has a similar chemical composition to the inorganic fraction of bovine bone and human and pig dental enamel and its FTIR spectrum is similar in the nu3 region to that of human and rodent bone mineral and dental enamel (2,17-18,30,39,42). Therefore, the structure of LM006 is probably a good approximation to the overall structure of CHAP in bone and enamel. All these materials are Na-bearing AB-CHAP, and their infrared spectra are characterized by nu3 band absorption confined more-or-less to the 1400-1500 cm^{-1} spectral interval.

An important feature of the study on synthetic Na-bearing CHAP (30) is that the proportion of A and B carbonate has been determined independently of the corresponding FTIR spectra (Figure 7) using single-crystal X-ray structure refinement. The criterion established in the literature supporting dominance by B carbonate in biological apatite based on the absence of significant nu3 absorption intensity beyond 1500 cm^{-1} has to be reconsidered in light of this study, which shows that the position of the nu3 band for type A carbonate in FTIR spectra of AB-CHAP, -CFAP and -CCLAP is shifted uniformly to lower wavenumber by the introduction of Na.

This conclusion is now reinforced by the nu2 band region of biological apatite, which better reflects the

true proportions of the principal carbonate species in CHAP (24; Figure 5). In biological apatite the nu2 region is normally deconvoluted to give singlet bands at 878 cm^{-1} (A carbonate), 871 cm^{-1} (B carbonate), and 866 cm^{-1} (labile carbonate; e.g. 17-18). Rey and coworkers reported B/A ratios from nu2 region spectra ranging from 1.1 to 0.8 for pig enamel (18) and 1.4 to 1.2 for various bone samples (cow, human, chicken, rat, and rabbit; 17,19). These results are independent confirmation that these biological apatites are all AB-CHAP and not dominantly B-CHAP.

We recognize that, although the overall structure of crystalline biological apatite appears to have been reproduced, the present synthetic CHAP crystals differ markedly from bone mineral in respect to crystal size, reactivity of the surface hydrated layer, and absence of HPO_4^{2-} (e.g. 17,19,39,44). Also, although the apatite species of bone is generally understood to be CHAP, structurally-bound hydroxyl is commonly not detected by spectroscopic studies (including infrared, Raman, and nuclear magnetic resonance) on mineralized tissue extracted from bone (e.g. 43). The present study has shown that the absence of the sharp OH stretch and libration bands is a characteristic feature in biological apatite and is not an artifact of the procedures used for processing mineralized tissues from mammals (20,42).

Obviously, the intensity of the infrared OH stretch and libration bands is also diminished by the entry of A carbonate ions and molecular H_2O into the channel, but the complete suppression of both OH stretch and OH libration bands indicates that any OH content present must be disordered in respect to its orientation and precise location. In CHAP, the proton is bound by only a single bond to the channel oxygen atom and, therefore, is readily deflected from its axial location by local change in the composition and structure of the channel wall. Note that hydrogen bonding is weak in HAP due to long O…O interactions (0.305 to 0.345 nm) and unfavorable O-H…O bond angles (e.g. 88.7, 107.2 degrees to O3) and unlikely to be a stabilizing factor. On the other hand, the carbonate ion is bound firmly by six or seven Ca2-O bonds in A-CHAP (Figure 3) and the FTIR spectra show that its overall orientation, with two oxygen atoms close to the *c*-axis, is retained, even for imperfectly crystallized CHAP with disordered hydroxyl.

In summary, interpretation of the infrared spectra of Na-bearing CHAP using X-ray structure site occupancies has led to the important conclusion that the proportion of channel carbonate in biological apatite is significantly higher than previously estimated. In fact, given that the channel constituents are readily exchangeable, it is now quite probable that a significant fraction of the labile fraction of carbonate in biological apatite, which has an important role in mediating acid-base reactions in the body (45), resides in the apatite channel (24,46).

It is emphasized that synthetic Na-bearing AB-CHAP with formula contents of A and B carbonate of about 0.5 (e.g., experiment LM006, Table 1; Fleet and Liu 2007) is similar in both chemical composition and FTIR spectrum to biological apatite. This agreement confirms that the quenched Na-bearing high-pressure CHAP products with channel (A) carbonate oriented with two oxygen atoms near the *c*-axis and structural (B) carbonate close to a sloping face of the PO_4 tetrahedron are appropriate analogues for the overall structural features of biological apatite. It is not too surprising that the basic structure of biological apatite is reproduced by high-pressure synthesis, given the extensive pressure-temperature stability field of apatite. In the present study, high temperature was required to yield crystals of a size and quality suitable for X-ray structure analysis and high pressure to confine CO_2-rich fluid and vapor. No phase changes were detected: rather, differences in structural details between the synthetic and biological apatites are thought to be limited to disorder related to low degree of crystallinity and OH and molecular water in the latter, as well as possible monohydrogenphosphate content, nanoscale crystal size and surface reactivity .

5. ACKNOWLEDGEMENTS

I thank Xi Liu and Xiaoyang Liu for high-pressure synthesis and collection of FTIR spectra, and the Natural Sciences and Engineering Research Council of Canada for financial support.

6. REFERENCES

1. Y Pan and M E Fleet: Compositions of the apatite-group minerals: Substitution mechanisms and controlling factors. In: Phosphates. Eds: Kohn M J Rakovan J Hughes J M. *Reviews in Mineralogy and Geochemistry* 48, 13-49, Mineralogical Society of America, Washington, D.C. (2002)

2. J C Elliott: Calcium phosphate biominerals. In: Phosphates. Eds: Kohn M J Rakovan J Hughes J M. *Reviews in Mineralogy and Geochemistry* 48, 427-453, Mineralogical Society of America, Washington, D.C. (2002)

3. F Brudevold D E Gardner F A Smith: Distribution of fluorine in human enamel. *J Dental Res* 35, 420-429 (1956)

4. G H McClellan J R Lehr: Crystal chemical investigation of natural apatites. *Am Mineral* 54, 1374-1391 (1969)

5. Xi Liu S R Shieh M E Fleet L Zhang Q He: Equation of state of carbonated hydroxylapatite at ambient temperature up to 10 GPa: Significance of carbonate. *Am Mineral* 96, 74-80 (2011)

6. J M Hughes J Rakovan:(2002) The crystal structure of apatite, $Ca_5(PO_4)_3(F,OH,Cl)$. In: Phosphates. Eds: Kohn M J Rakovan J Hughes J M. *Reviews in Mineralogy and Geochemistry* 48, 1-12, Mineralogical Society of America, Washington, D.C. (2002)

7. J M Hughes M Cameron K D Crowley: Structural variations in natural F, OH, and Cl apatites. *Am Mineral* 74, 870-876 (1989)

8. J C Elliott: Structure and Chemistry of the Apatites and Other Calcium Orthophosphates, 389 p, Elsevier, Amsterdam (1994)

9. Y Suetsugu Y Takahashi F P Okamura J Tanaka: Structure analysis of A-type carbonate apatite by a single-crystal X-ray diffraction method. *J Solid State Chem* 155, 292-297 (2000)

10. T I Ivanova O V Frank-Kamenetskaya A B Kol'tsov V L Ugolkov: Crystal structure of calcium-deficient carbonated hydroxyapatite. Thermal decomposition. *J Solid State Chem* 160, 340-349 (2001)

11. R M Wilson J C Elliott S E P Dowker R I Smith: Rietveld structure refinement of precipitated carbonate apatite using neutron diffraction data. *Biomaterials* 25, 2205-2213 (2004)

12. Th Leventouri B C Chakoumakos H Y Moghaddam V Perdikatsis: Powder neutron diffraction studies of a carbonate fluorapatite. *J Materials Res* 15, 511-517 (2000)

13. T Tonegawa T Ikoma T Yoshioka N Hanagata J Tanaka: Crystal structure refinement of A-type carbonate apatite by X-ray powder diffraction. *J Materials Sci* 45, 2419-2426 (2010)

14. J C Elliott: The interpretation of the infra-red absorption spectra of some carbonate-containing apatites. In: Tooth Enamel: Its Composition, Properties, and Fundamental Structure. Eds: Fearnhead R W Stack M V. pp. 20-22. John Wright & Sons Bristol, UK. (1964)

15. G Bonel: Contribution à l'étude de la carbonatation des apatites. I. Synthèse et étude des propriétés physico-chimiques des apatites carbonatées du type A. *Annales de Chimie (Paris)* 7, 65-88 (1972)

16. R Z LeGeros O R Trautz E Klein J P LeGeros:Two types of carbonate substitution in the apatite structure. *Experimentia* 25, 5-7 (1969)

17. C Rey B Collins T Goehl I R Dickson M J Glimcher: The carbonate environment in bone mineral: A resolution-enhanced Fourier transform infrared study. *Calcif Tissue Int* 45, 157-164 (1989)

18. C Rey V Renugopalakrishnan M Shimizu B Collins M J Glimcher: A resolution-enhanced Fourier transform infrared spectroscopic study of the environment of the CO_3^{2-} ion in the mineral phase of enamel during its formation and maturation. *Calcif Tissue Int* 49, 259-268 (1991)

19. H-M Kim C Rey M J Glimcher: X-ray diffraction, electron microscopy, and Fourier transform infrared spectroscopy of apatite crystals isolated from chicken and bovine calcified cartilage. *Calcif Tissue Int* 59, 58-63 (1996)

20. G Cho Y Wu J L Ackerman: Detection of hydroxyl ions in bone mineral by solid state NMR spectroscopy. *Science (Wash)* 300, 1123-1127 (2003)

21. H E Mason A Kozlowski B L Phillips: Solid-state NMR study of the role of H and Na in AB-type carbonate hydroxylapatite. *Chem Materials* 20, 294-302 (2007)

22. M E Fleet X Liu P L King: Accommodation of the carbonate ion in apatite: An FTIR and X-ray structure study of crystals synthesized at 2-4 GPa. *Am Mineral* 89, 1422-1432 (2004)

23. R C Tacker: Carbonate in igneous and metamorphic fluorapatite: Two type A and two type B substitutions. *Am Mineral* 93, 168-176 (2008)

24. M E Fleet: Infrared spectra of carbonate apatites: nu2-region bands. *Biomaterials* 30, 1473-1481 (2009)

25. A Peeters E A P De Maeyer C Van Alsenoy R M H Verbeeck: Solids modeled by ab initio crystal-field methods. 12. Structure, orientation and position of A-type carbonate in a hydroxyapatite lattice. *J Phys Chem* B 101, 3995-3998 (1997)

26. S Peroos Z Du N H de Leeuw: A computer modelling study of the uptake, structure and distribution of carbonate defects in hydroxyapatite. *Biomaterials* 27, 2150-2161 (2006)

27. M E Fleet X Liu: Carbonate apatite type A synthesized at high pressure: new space group (*P*-3) and orientation of channel carbonate ion. *J Solid State Chem* 174, 412-417 (2003)

28. M E Fleet X Liu: Location of type B carbonate ion in type A-B carbonate apatite synthesized at high pressure. *J Solid State Chem* 177, 3174-3182 (2004)

29. M E Fleet X Liu: Local structure of channel ions in carbonate apatite. *Biomaterials* 26, 7548-7554 (2005)

30. M E Fleet Xi Liu: Coupled substitution of type A and B carbonate in sodium-bearing apatite. *Biomaterials* 28, 916-926 (2007)

31. M E Fleet Xi Liu: Accommodation of the carbonate ion in fluorapatite synthesized at high pressure. *Am Mineral* 93, 1460-1469 (2008)

32. M E Fleet Xi Liu: Type A-B carbonate chlorapatite synthesized at high pressure. *J Solid State Chem* 181, 2494-2500 (2008)

33. Nonius, COLLECT Software. Bruker-Nonius, Delft, The Netherlands (1997)

34. Siemens SHELXTL PC, Version 4.1, Siemens Analytical X-ray Instruments, Inc., Madison, WI, USA (1993)

35. P Coppens, LINEX77, State University of New York, Buffalo, USA (1977)

36. International Tables for X-ray Crystallography, Vol. IV. Eds. Ibers J A. Hamilton W C. Kynoch Press, Birmingham, UK (1974)

37. M E Fleet X Liu Xi Liu: Orientation of channel carbonate ions in apatite: Effect of pressure and composition. *Am Mineral* 96, 1148-1157 (2011)

38. H Morgan R M Wilson J C Elliott S E P Dowker P Anderson: Preparation and characterization of monoclinic hydroxyapatite and its precipitated carbonate apatite intermediate. *Biomaterials* 21, 617-627 (2000)

39. D Farlay G Panzcer C Rey P D Delmas G Boivin: Mineral maturity and crystallinity index are distinct characteristics of bone mineral. *J Bone Miner Met* 28, 433-445 (2010)

40. D G A Nelson B E Williamson: Low-temperature laser Raman spectroscopy of synthetic carbonated apatites and dental enamel. *Aust J Chem* 35, 715-727 (1982)

41. T Ikoma A Yamazaki S Nakamura M. Akao: Preparation and structure refinement of monoclinic hydroxyapatite. *J Solid State Chem* 144, 272-276 (1999)

42. S Aparicio S B Doty N P Camacho E P Paschalis L Spevak R Mendelsohn A L Boskey: Optimal methods for processing mineralized tissues for Fourier transform infrared microspectroscopy. *Calcif Tissue Int* 70, 422-429 (2002)

43. B Wopenka J D Pasteris: A mineralogical perspective on the apatite in bone. *Materials Sci Engin* C25, 131-143 (2005)

44. A L Boskey: Mineral analysis provides insights into the mechanism of biomineralization. *Calcif Tissue Int* 72, 533-536 (2003)

45. D A Bushinsky S B Smith K L Gavrilov L F Gavrilov J Li R Levi-Setti: Acute acidosis-induced alteration in bone bicarbonate and phosphate, *Am J Physiol- Renal Physiol* 283, F1091-F1097 (2002)

46. H R Low C Ritter T J White: Crystal structure refinements of the 2*H* and 2*M* pseudomorphs of ferric carbonate-hydroxyapatite. *Dalton Trans* 39, 6488-6495 (2010)

Key Words Apatite structure, Carbonate hydroxyapatite, X-ray structure, Infrared spectroscopy, Biomineralisation, CO_2 sequestration

Send correspondence to: Michael E. Fleet, Department of Earth Sciences, University of Western Ontario, London, Ontario N6A 5B7, Canada, Tel: 519-661-2253, Fax- 519-661-3198, E-mail: mfleet@uwo.ca